



10-3-2012

High-frequency ultrasound M-mode monitoring of HIFU ablation in cardiac tissue

Ronald Kumon
Kettering University

Madhu Sudhan Reddy Gudur
University of Michigan

Yun Zhou
University of Michigan-Ann Arbor

Cheri X. Deng
University of Michigan

Follow this and additional works at: https://digitalcommons.kettering.edu/physics_conference

 Part of the [Physics Commons](#)

Recommended Citation

Kumon, Ronald; Gudur, Madhu Sudhan Reddy; Zhou, Yun; and Deng, Cheri X., "High-frequency ultrasound M-mode monitoring of HIFU ablation in cardiac tissue" (2012). *Physics Presentations And Conference Materials*. 4.
https://digitalcommons.kettering.edu/physics_conference/4

This Article is brought to you for free and open access by the Physics at Digital Commons @ Kettering University. It has been accepted for inclusion in Physics Presentations And Conference Materials by an authorized administrator of Digital Commons @ Kettering University. For more information, please contact digitalcommons@kettering.edu.

High-Frequency Ultrasound M-mode Monitoring of HIFU Ablation in Cardiac Tissue

R. E. Kumon^{a,b}, M. S. R. Gudur^a, Y. Zhou^a, and C. X. Deng^a

^a*Department of Biomedical Engineering, University of Michigan,
2200 Bonisteel Blvd., Ann Arbor, MI 48109-2099, USA*

^b*Department of Physics, Kettering University, 1700 University Ave., Flint, MI 48504-6214, USA*

Abstract. Effective real-time HIFU lesion detection is important for expanded use of HIFU in interventional electrophysiology (e.g., epicardial ablation of cardiac arrhythmia). The goal of this study was to investigate rapid, high-frequency M-mode ultrasound imaging for monitoring spatiotemporal changes in tissue during HIFU application. The HIFU application (4.33 MHz, 1000 Hz PRF, 50% duty cycle, 1 s exposure, 6100 W/cm²) was perpendicularly applied to porcine cardiac tissue with a high-frequency imaging system (Visualsonics Vevo 770, 55 MHz, 4.5 mm focal distance) confocally aligned. Radiofrequency (RF) M-mode data (1 kHz PRF, 4 s x 7 mm) was acquired before, during, and after HIFU treatment. Gross lesions were compared with M-mode data to correlate lesion and cavity formation. Integrated backscatter, echo-decorrelation parameters, and their cumulative extrema over time were analyzed for automatically identifying lesion width and bubble formation. Cumulative maximum integrated backscatter showed the best results for identifying the final lesion width, and a criterion based on line-to-line decorrelation was proposed for identification of transient bubble activity.

Keywords: Cardiac Ablation, Tissue Characterization, High-Frequency Ultrasound, HIFU

PACS: 43.80.Sh, 43.80.Qf, 87.50.Y-, 87.63.D-, 87.57.-s

INTRODUCTION

High-intensity focused ultrasound (HIFU) ablation is an emerging therapeutic modality that has been applied in a variety of clinical contexts¹, including ablation of cardiac tissue for treatment of cardiac arrhythmia². Radio-frequency (RF) electrical, microwave, laser, cryo-therapies have been exploited for cardiac ablation, but current technologies are sub-optimal, mainly due to their limited ability to create linear transmural lesions desired during treatment with minimum collateral damage³. Relative to these methods, HIFU is a non-invasive method with adjustable depth penetration. However, effective real-time treatment monitoring remains a challenge.

The purpose of this study is to develop methods for real-time, automated identification of lesion extent and gas body formation using high-frequency ultrasound. Towards this end, we compute integrated backscatter and echo-decorrelation parameters from radiofrequency (RF) rapid M-mode ultrasound data, based on previous results using these parameters to monitor RF electrical ablation⁴. We hypothesize that the cumulative time history of these parameters will better reflect the extent tissue necrosis than the individual parameters alone. The resulting parametric images are then compared against gross lesion photographs to develop a

criterion for lesion identification. Based on our observations, we also propose a criterion for identification of newly created or moving gas bodies based on a line-to-line echo decorrelation parameter.

MATERIALS AND METHODS

Figure 1 shows a schematic diagram of the experimental setup. Lesions were generated by a HIFU system consisting of a signal generator (Agilent 33220A, Santa Clara, CA, USA), power amplifier (Amplifier Research 75A250, Souderton, PA, USA), and HIFU transducer (4.33 MHz center freq.). Real time monitoring of HIFU application was performed by employing a high-frequency ultrasound imaging system (Vevo 770, Visualsonics, Toronto, ON, Canada) and a scanhead with a center frequency of 55 MHz (RMV 708, 4.5 mm focal distance, 1.5 mm depth of focus [−6 dB]). The HIFU transducer and scanhead were perpendicular to each other in a common plane (imaging plane) with approximately the same focus. The resulting RF signals during M-mode imaging were acquired by a digitizing oscilloscope (Agilent 54830B, Santa Clara, CA, USA, with 8-bit dynamic range, 500 Ms/s) from the RF output of the Vevo system. The freshly-excised porcine ventricular cardiac tissue specimens received HIFU exposure (50% duty cycle, 1 kHz pulse repetition frequency [PRF], 1 s total duration, focal acoustic intensity 6100 W/cm²). M-mode imaging (1 kHz PRF, 4 s x 7 mm) was performed 0.2 s before, 1 s during, and 2.8 s after HIFU treatment for total imaging duration of 4 s. The M-mode imaging line was placed at the location of the HIFU focus. To prevent interference between the HIFU and M-mode imaging pulses, a custom timing circuit used the RF line trigger output from the Vevo 770 to properly synchronize imaging with the HIFU pulses with the imaging.

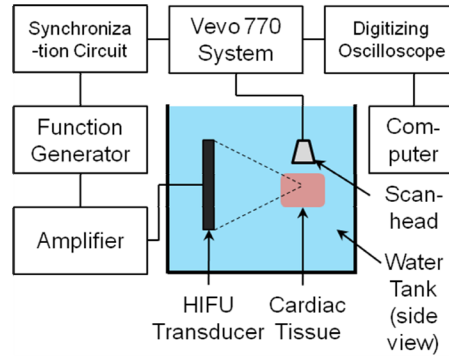


FIGURE 1. Schematic diagram of experimental apparatus.

The data analysis was performed by importing the RF data from the Vevo into MATLAB. Let $q(z, t)$ be the real-valued M-line signal from the Vevo at time t at range $z = ct'/2$, where c is sound speed and t' is echo arrival time, and let $p(z, t) = H[q(z, t)]$ be its Hilbert transform. The change in the integrated backscatter (IBS) relative to the initial IBS was defined as⁴

$$\Delta IBS(y, z, t) = 10 \log_{10} \left[R_0(z, t) / R_0(z, 0) \right], \quad R_0(z, t) = \left\langle |p(z, t)|^2 \right\rangle, \quad (1)$$

where a spatially averaging function is defined as

$$\langle f(z,t) \rangle = \int w(z-z_0) f(z_0,t) dz_0, \quad w(z) = \exp(-z^2/2\gamma^2) \quad (2)$$

with $\gamma = 16.6 \mu\text{m}$. The line-to-line⁴ and initial-to-current-line echo-decorrelation parameters were defined as

$$\sigma(z,t) = \frac{|R_0(z,t) - |R(z,t,\tau)||}{\frac{1}{2}[R_0(z,t) + \overline{R_0(t)}]}, \quad \sigma_l(z,t) = \frac{|R_0(z,t) - |R_l(z,t)||}{\frac{1}{2}[R_0(z,t) + \overline{R_0(t)}]}, \quad (3)$$

respectively, where $R(z,t,\tau) = p(z,t)p^*(z,t+\tau)$ and $R_l(z,t) = \langle p(z,0)p^*(z,t) \rangle$. For any given parameter $X(z,t)$ defined above, its temporal cumulative maximum was computed according to the definition $X_{\max}(z,t) = \max_{t'} [X(z,0 \leq t' \leq t)]$.

RESULTS AND DISCUSSION

Figures 2A and 2B show typical B-mode images before and after HIFU application. M-mode imaging was performed along the direction of the dashed line. At this intensity level, a lesion was generated with a hypoechoic core with a surrounding hyperechoic region, relative to the tissue's initial state shown in Fig. 2A. Figure 2C shows the corresponding M-mode image reconstructed from the RF data, where the vertical dashed lines indicate the times that the HIFU treatment was turned on and off ($t = 0.2 \text{ s}$ and 1.2 s). After the HIFU is turned on, no activity was seen until $t = 0.460 \text{ s}$, when a hyperechoic burst initiates in the focal area of the HIFU transducer. After this burst, the hypoechoic region moves upwards until $t \sim 0.8 \text{ s}$ but gradually weakens and nearly disappears. This behavior suggests that bubbles generated at the focus may move upwards as the cavity expands but this gas either dissolves back into the tissue

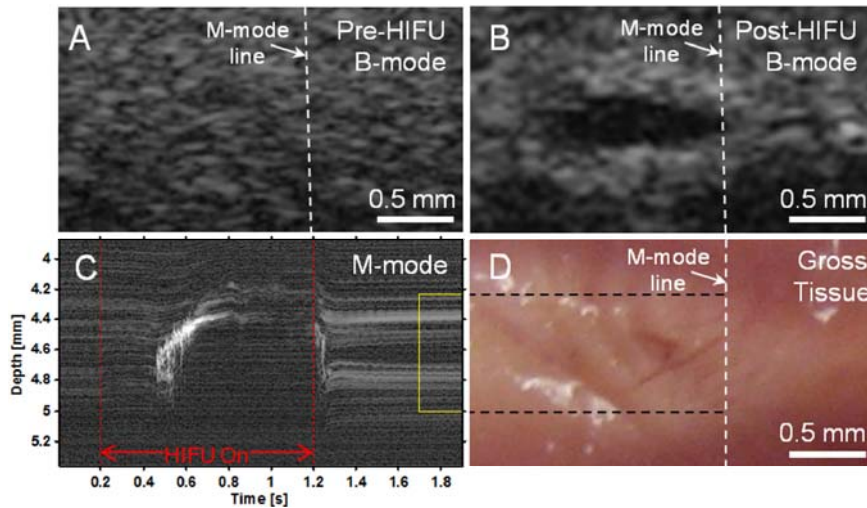


FIGURE 2. (A) Pre-HIFU and (B) post-HIFU B-mode images of lesion with corresponding (C) M-mode image during HIFU application and (D) photograph of gross tissue with lesion.

or moves into other parts of the cavity away from the M-mode line. After the HIFU is turned off, there is an apparent transverse relaxation of the tissue followed by the appearance of a hypoechoic core corresponding to the generated cavity.

To test the accuracy of each parameter in identifying the lesion region, M-mode images were constructed for each parameter. For any given parametric image, a threshold θ can be applied to classify each pixel as lesion or non-lesion if the parameter is above or below the threshold. Based on the images of the gross lesion, each pixel in the image was classified. By using a series of thresholds, an overall empirical receiver-operating characteristic (ROC) curve was formed for each parameter, and then the area under the ROC curve (AUC) was computed as an overall measure of the parameter's performance. An empirical accuracy curve was also constructed as function of θ . An optimal threshold θ_0 was defined as the lowest threshold corresponding to the maximum accuracy. To allow time for the system to equilibrate, only the M-lines starting 0.5 s after HIFU termination were classified.

As a specific example of the method, Fig. 3 shows the resulting ROC curves for the specimen in Fig. 2. The cumulative maximum change in the integrated backscatter ΔIBS_{\max} showed the best performance with AUC = 0.971 and had a maximum accuracy of 0.91 at the threshold 9.5 dB (Fig. 4C). In general, the cumulative maximum parameters performed as good or better than the corresponding parameter by itself for lesion identification.

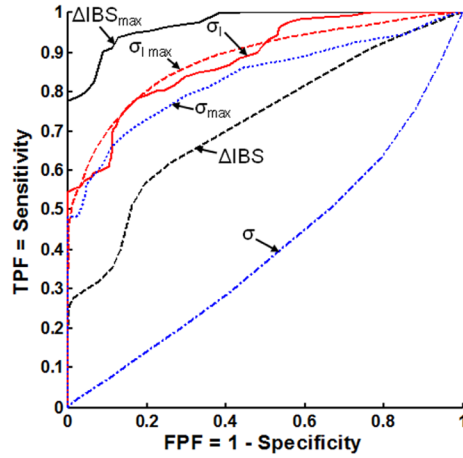


FIGURE 3. Receiver operating characteristic curves for ΔIBS_{\max} (solid black), ΔIBS (dashed black), $\sigma_{I \max}$ (dashed red), σ_I (solid red), σ_{\max} (dotted blue), and σ (dashed-dotted blue) for data shown in Fig. 2.

Figure 4 provides a graphical illustration of the pixel marking process using ΔIBS_{\max} for lesion identification. Fig. 4A shows the parametric image map of ΔIBS , while Fig. 4B shows the corresponding cumulative maximum ΔIBS_{\max} . The yellow box vertically delineates the estimated spatial region where the lesion was formed based on examination of the gross lesion (Fig. 2D) and horizontally delineates the temporal duration from 0.5 s to 0.7 s after the HIFU was turned off, when the tissue has reached an approximate equilibrium state. Fig. 4C shows the lesion classification accuracy as a function of ΔIBS_{\max} threshold with the peak value occurring at 9.5 dB (dashed line). By applying this threshold to Fig. 4B, a binary mask was generated

(Fig. 4D), where red indicates lesion and black indicates non-lesion. Around $t = 0.726$ s, there is an abrupt increase in the width of the identified lesion region, possibly due to an increase in backscatter due to more extensive bubble activity and/or macroscopic cavity generation.

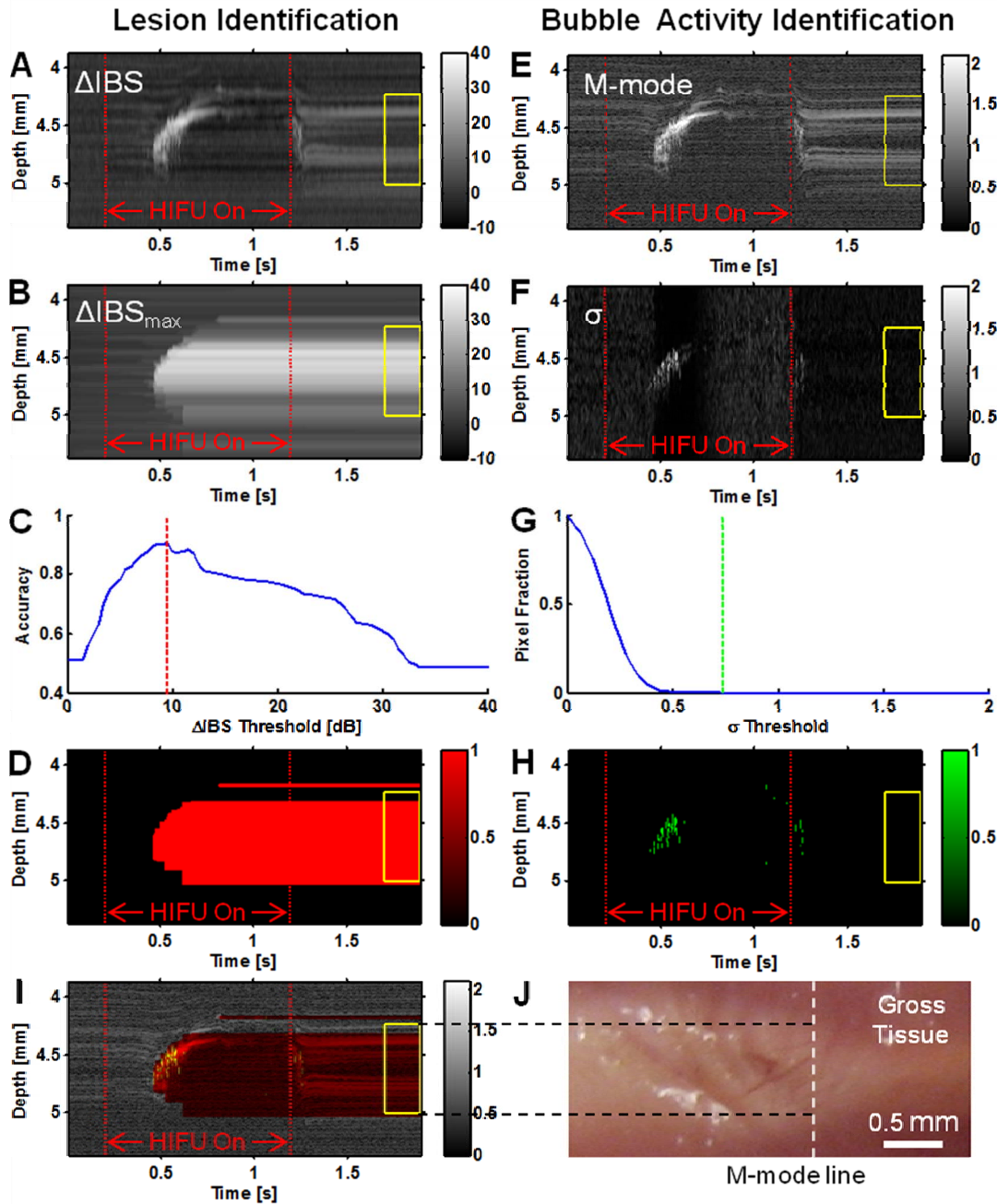


FIGURE 4. Graphical illustration of algorithm for marking (A–D) lesion extent and (E–H) probable bubble activity with comparison of (I) composite grayscale M-mode image and (J) photo of gross lesion. In the composite, red indicates lesion, green indicates bubble, and yellow indicates both.

Because gas bodies that are generated by cavitation or boiling will likely be transient events, we proposed to identify bubble activity or motion by using the frame-to-frame decorrelation parameter σ . Comparison of the grayscale M-mode image (Fig. 4E) with the corresponding parametric image map of σ (Fig. 4F) shows high values of decorrelation in the same hyperechoic areas where the bubble activity was likely to have occurred. Because no HIFU-associated bubbles are likely to exist within the tissue prior to HIFU initiation, any parameter used for classification of bubble activity should, at minimum, not identify bubbles during the pre-HIFU period. By examining the pixel fraction above any given threshold value in the pre-HIFU region (Fig. 4G), we determined that a threshold $\sigma_0 = 0.74$ was sufficient large for this cases to ensure that no pixels would be identified before HIFU. Figure 4H shows a binary map generated using this criterion, where green indicates bubble activity and black indicates non-bubble activity.

Figure 4I then shows the composite of the grayscale M-mode image (Fig. 4E), lesion mask (Fig. 4B), and bubble-activity mask (Fig. 4H), where red indicates lesion only, green indicates bubble activity only, and yellow indicates the superposition of both. For ease of comparison, Fig. 4J (same as Fig. 2D) shows the image of the gross lesion with the approximate location of the M-mode imaging indicated by the dashed vertical line. Observe that the grayscale M-mode image does not clearly identify the extent of the lesion region, whereas the masks provide good automated marking of the lesion extent and probable bubble activity along the M-mode line.

CONCLUSION

We have demonstrated a method to identify the lesion extent using the time history of rapid, high-frequency M-mode imaging to compute the temporal cumulative maximum integrated backscatter. We also proposed a criterion for identification of transient bubble activity based on a line-to-line decorrelation parameter. Implementation of these techniques can provide rapid assessment for HIFU ablation. Additional work is currently ongoing to examine addition specimens under other HIFU excitation conditions (e.g., different focal intensities) and evaluate additional parameters (e.g., spectral parameters like mid-band fit, intercept, and slope⁵).

This work was supported by the National Institutes of Health (grant R01 EB008999) and the University of Michigan.

REFERENCES

1. G. ter Haar, *Prog Biophys Mol Biol* **93** (1-3), 111-129 (2007).
2. S. Schopka, C. Schmid, A. Keyser, A. Kortner, J. Tafelmeier, C. Diez, L. Rupprecht and M. Hilker, *Journal of Cardiothoracic Surgery* **5** (2010).
3. A. M. Gillinov, G. Pettersson and T. W. Rice, *J Thorac Cardiovasc Surg* **122** (6), 1239-1240 (2001).
4. T. D. Mast, D. P. Pucke, S. E. Subramanian, W. J. Bowus, S. M. Rudich and J. F. Buell, *J. Ultrasound Med.* **27** (12), 1685-1697 (2008).
5. F. L. Lizzi, M. Astor, T. Liu, C. Deng, D. J. Coleman and R. H. Silverman, *Int J Imag Syst Tech* **8** (1), 3-10 (1997).

Copyright of AIP Conference Proceedings is the property of American Institute of Physics and its content may not be copied or emailed to multiple sites or posted to a listserv without the copyright holder's express written permission. However, users may print, download, or email articles for individual use.